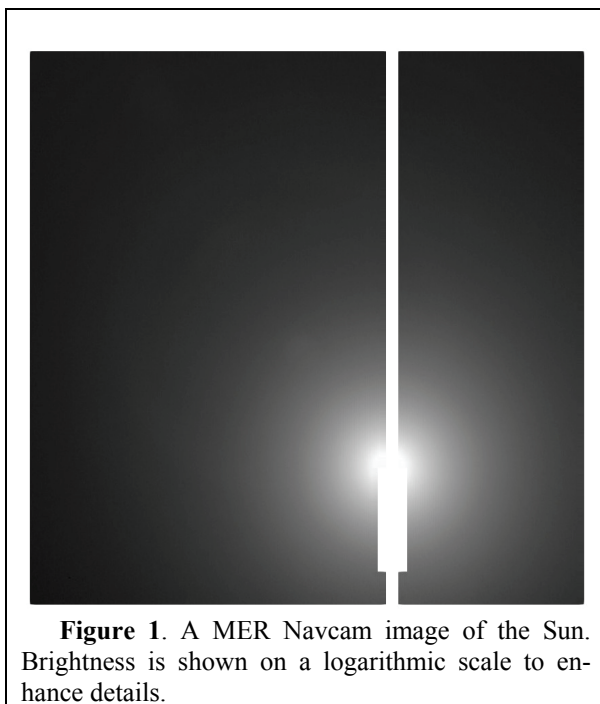# DUST AEROSOL PARTICLE SIZE AND SHAPE USING MER NAVCAM AND PANCAM SKY IMAGING

Michael D. Smith , *NASA Goddard Space Flight Center, Greenbelt, MD, USA (Michael.D.Smith@nasa.gov)*, **Michael J. Wolff**, *Space Sciences Institute, Boulder, CO, USA.*

Introduction: Imaging of the sky taken by the Navcam (Maki *et al.*, 2003) and Pancam (Bell *et al.*, 2003) cameras on-board the Mars Exploration Rovers (MER) provide a useful tool for determining the optical depth and physical properties of aerosols above the rover (Lemmon *et al.*, 2004; Soderblom *et al.*, 2008). Specifically, the brightness of the sky as a function of angle away from the Sun can strongly constrain the size distribution and shape of dust and water ice aerosols. This technique is also directly applicable to images of the Sun and sky taken by the Mars Science Laboratory (MSL) Mastcam and Navcam cameras, or any other rover- or lander-based camera.
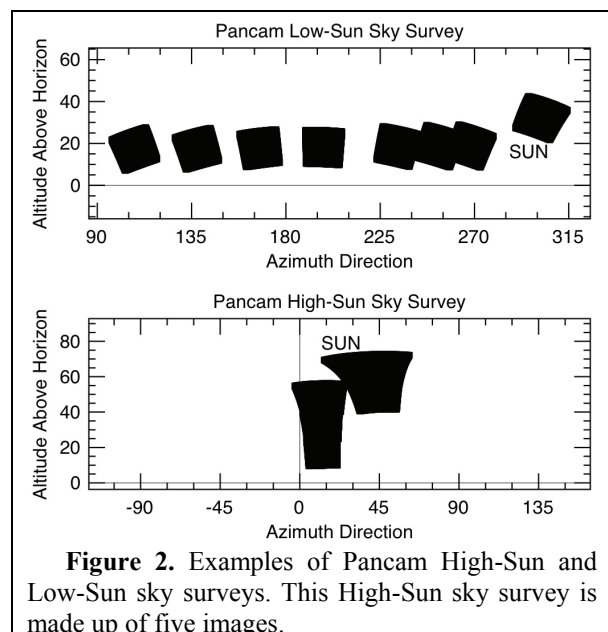
Data Set: Hundreds of Navcam images of the Sun and Pancam "sky surveys" have been taken by each of the two MER rovers covering a total time span of several Mars years and a wide range of dust loading conditions including the planet-encircling dust storm during Mars Year 28 (Earth Year 2007).

Figure 1. A MER Navcam image of the Sun. Brightness is shown on a logarithmic scale to enhance details.

Navcam images (650 nm effective wavelength) of the Sun are taken as a single frame with the Sun located toward one side (Figure 1). The 45° x 45° Navcam field of view permits sampling of the scattering phase function from very near the Sun to 30°–35° away from the Sun. Because the Navcam instrument design minimizes internal instrumental scattered light, reliable measurements can be ob-

served to within just a few degrees of the Sun. These observations of near-Sun scattering are very well suited for the retrieval of aerosol particle size.

Pancam sky imaging has been used to create "sky surveys" that cover a wide range of scattering angles at several wavelengths between 430 and 1000 nm. Because the Pancam field of view is 16° x 16°, each sky survey is made up of several images in order to cover a broad swath across the sky (Figure 2). There are two major classes of Pancam sky surveys. The first, "Low-Sun sky survey," are taken when the Sun is low in the sky, typically 15°–30° above the horizon. A sequence of images is taken to cover a wide range of azimuths at the altitude of the Sun. The second class of sky survey, "High-Sun," is taken when the Sun is high in the sky (elevation angle ~65°–85°). Starting near the Sun, the sequence moves the field of view downward toward the horizon. Because of the wide range of scattering angles that they cover, the Pancam sky surveys generally offer greater utility than the Navcam observations for constraining particle shape information.

Figure 2. Examples of Pancam High-Sun and Low-Sun sky surveys. This High-Sun sky survey is made up of five images.
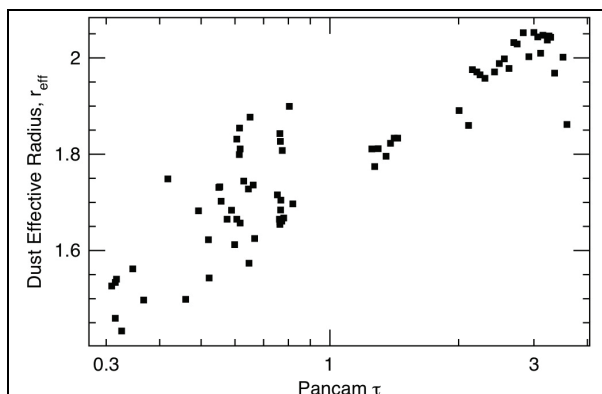
Both the Navcam and the Pancam observations were taken systematically throughout the MER mission, and continue to be taken by *Opportunity*.

Retrieval: Multiple scattering radiative transfer modeling is used to model the upward-looking observations. In this geometry, the observed sky brightness comes from sunlight scattered by aerosols into the line-of-sight of each pixel, and thus depends

primarily on a few basic quantities: aerosol optical depth, vertical distribution, and angular scattering properties. By excluding observations very near the horizon, we reduce the importance of the vertical distribution of aerosols, and we assume a well-mixed aerosol for simplicity. For the purpose of treating only dust, we also avoid any images with obvious water ice clouds. The radiative transfer model employed is a discrete-ordinates code that we have used previously in the analysis of CRISM and other Mars spacecraft data (*e.g.*, Smith *et al.*, 2009; 2013).

For the retrieval of dust particle size using Navcam images, we assume the dust optical constants derived by Wolff *et al.* (2009), and a modified gamma dust particle size distribution (*e.g.,* Hansen and Travis, 1974) with effective variance, $v_{eff} = 0.3$. Column optical depth of dust can in principle be retrieved from the Navcam images directly, but it is advantageous for this study to remove that free parameter and use the very accurate values retrieved from direct imaging of the Sun by Pancam on a daily basis (Lemmon *et al.*, 2004). This leaves the effective dust particle size, r_{eff}, as the remaining free parameter. Scattering phase functions are computed using the dust optical properties and the particle size distribution (r_{eff}, v_{eff}) values using a T-matrix code (Mishchenko *et al.*, 2000), with dust modeled as cylinders with a length-to-diameter ratio of unity.
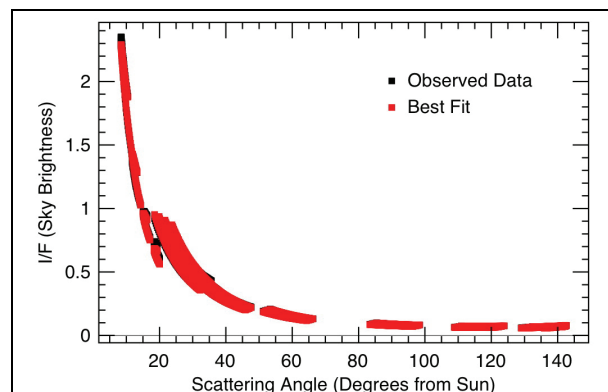

Figure 3. The effective radius of dust particles retrieved from Navcam images of the Sun and surrounding sky by *Spirit* as a function of column optical depth derived from direct imaging of the Sun by Pancam.
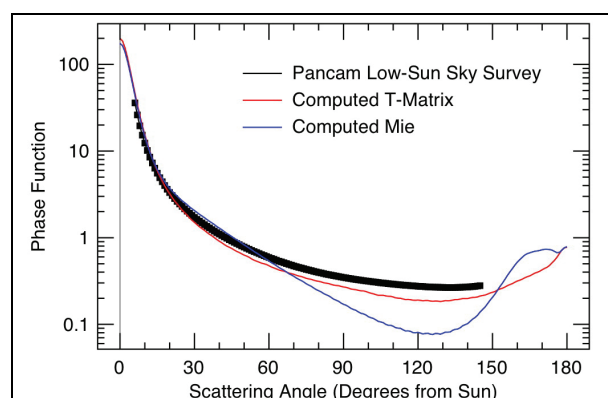
To model the Pancam sky surveys we have taken a somewhat different approach. In this case we wish to constrain particle shape, so we make no assumptions about the size or optical properties of the dust. Instead, we directly retrieve the scattering phase function that produces the best fit to the observed data. The only assumptions are the column optical depth (determined in a separate step using the Pancam direct imaging of the Sun that is included with every sky survey) and that the scattering particles are uniform and well-mixed throughout the atmosphere. Once the scattering phase function has

been retrieved from the observations, information on particle size and shape can be obtained by computing phase functions with different models for dust (varying r_{eff}, v_{eff}, and shape) to see which best reproduce the retrieval.

Results: Figure 3 shows the retrieved dust particle effective radius, r_{eff}, for a sample of Navcam images taken by *Spirit* covering more than two Mars years including the MY 28 global-scale dust storm. The results show a clear trend for larger dust particles when the column optical depth of dust is highest. The injection of larger dust particles into the atmosphere during the active phase of a large dust storm is not a surprising result, but quantification of the effect is useful. The retrieved range of effective radii, between roughly 1.45 and 2.05 μm, is consistent with previous analyses (*e.g.*, Wolff and Clancy, 2003; Wolff *et al.*, 2006; Clancy *et al.*, 2003).
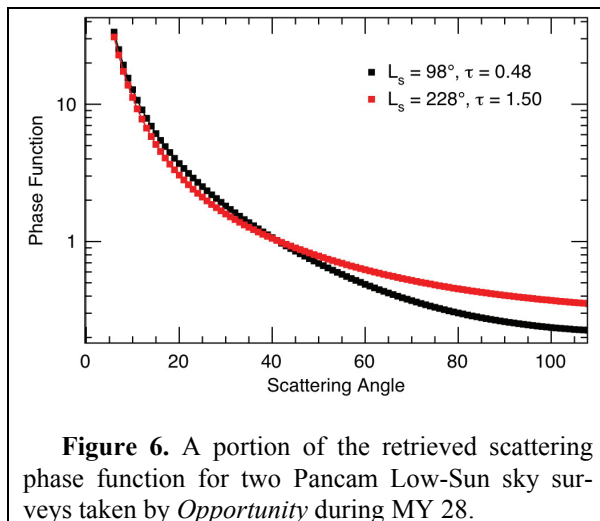

Figure 4. A typical Pancam Low-Sun sky survey taken by *Opportunity* (MY 27, Ls = 98°, dust optical depth = 0.48), and the best fit to the data. Note the wide range of scattering angles covered.

Figure 5. The scattering phase function retrieved from *Spirit* (MY 26, Ls = 354°, dust optical depth = 0.77) compared against models computed using T-matrix (D/L = 1 cylinders) and Mie scattering with $r_{eff} = 1.5$ μm, $v_{eff} = 0.3$. Mie spheres do not provide a good match.

The degrees of freedom provided by retrieving the entire scattering phase function generally allows for an excellent fit to the observed data. Figure 4 shows an example of the fit to a Pancam Low-Sun sky survey taken by *Opportunity*. A unique phase function can easily be found that reproduces the more than an order of magnitude difference in sky brightness between scattering angles of 10° and 140°.

Figure 5 highlights a scattering phase function retrieved from another Low-Sun sky survey, this time from *Spirit* near equinox (thick black line). For comparison, we include two phase functions computed using the Wolff *et al.* (2009) dust optical constants and a modified gamma size distribution with effective radius r_{eff} = 1.5 μm and effective variance v_{eff} = 0.3. The red line shows the phase function of cylinders with a length-to-diameter ratio of unity (D/L = 1) computed using a T-matrix code, while the blue line shows the phase function computed using standard Mie theory for spherical particles. The forward scattering peak of the phase function (scattering angles less than 30°) is not particularly sensitive to particle shape. However, the backscattering peak and the structure at larger scattering angles, especially beyond 90°, do depend significantly on the specific assumptions made regarding the particles. In this case (and for all sky surveys that we have examined thus far), Mie scattering fails to provide a good description of the phase function for the observed range of scattering angles. Cylinders provide a much closer match, although the backscattering peak is likely too large.

Figure 6. A portion of the retrieved scattering phase function for two Pancam Low-Sun sky surveys taken by *Opportunity* during MY 28.

Phase functions retrieved from Low-Sun sky surveys also reflect the seasonal variations in particle size observed by Navcam. Figure 6 shows the phase functions derived from two Low-Sun sky surveys, one (shown in black) for a time during the aphelion season when column dust optical depth was near minimum and one (shown in red) for a time during the decay of the MY 28 global-scale dust storm. Alt-

hough the Pancam sky surveys cannot reach the very small scattering angles that are most diagnostic of particle size, there is still a clear difference between the two phase functions with the dusty phase function having a more narrow forward scattering peak, which is indicative of larger particles.

Only the Pancam Low-Sun sky surveys contain scattering angles greater than 90°, which are most diagnostic of particle shape information as seen in Figure 5. However, High-Sun sky surveys are much easier to schedule since they are taken in the middle of the day when rover power is relatively plentiful, and they are useful as a supplement to the Navcam Sun images. The Pancam sky surveys include images taken using several narrowband filters covering a wavelength range of 430 to 1000 nm. Analysis of the angular variation of sky brightness as a function of wavelength may help differentiate between dust and water ice aerosols, and can potentially provide further constraints on particle size and optical constants.

Summary: The seasonal variation of aerosol particle size and shape constraints can be determined from images of the sky taken by the Pancam and Navcam cameras on-board the Mars Exploration Rovers. We find that scattering from spheres is not a good approximation for describing the angular variation of sky brightness far from the Sun (at scattering angles greater than about 60°). Significant seasonal variations are seen in the retrieved effective radius of dust, with higher optical depth strongly correlated with larger particle size.

References:

Bell III, J. F., *et al.* (2003). *J. Geophys. Res.*, **108**, E12, 8063, doi:10.1029/2003JE002070.

Clancy, R. T., *et al.* (2003). *J. Geophys. Res.*, **108**, E9, 598, doi:10.1029/2003JE002058.

Hansen, J. E., and L. D. Travis (1974), *Space Sci. Rev.*, **16**, 527–610.

Lemmon, M. T., *et al.* (2004). *Science*, **306**, 1753–1756.

Maki, J. N., *et al.* (2003). *J. Geophys. Res.*, **108,** E12, 8071, doi:10.1029/2003JE002077.

Mishchenko, M. I., *et al.* (2000). *Light Scattering by Nonspherical Particles*, 690 pp., Academic Press, San Diego.

Smith, M. D., *et al.* (2009). *J. Geophys. Res.*, **114**, E00D03, doi:10.1029/2008JE003288.

Smith, M. D., *et al.* (2013). *J. Geophys. Res.*, **118**, doi:10.1002/jgre.20047.

Soderblom, J. M., *et al.* (2008). *J. Geophys. Res.*, **113**, E06S19, doi:10.1029/2007JE003003.

Wolff, M. J., and R. T. Clancy (2003). *J. Geophys. Res.*, **108**, E9, 5097, doi:10.1029/2003JE002057.

Wolff, M. J., *et al.* (2006). *J. Geophys. Res.*, **111**, E12S17, doi:10.1029/2006JE002786.

Wolff, M. J., *et al.* (2009). *J. Geophys. Res.*, **114**, E00D04, doi:10.1029/2009JE003350.